Targeting CD19-positive lymphomas with the antibody-drug conjugate loncastuximab tesirine: preclinical evidence of activity as a single agent and in combination therapy

Chiara Tarantelli,[1]* David Wald,[2]* Nicolas Munz,[1] Filippo Spriano,[1] Alessio Bruscaggin,[1] Eleonora Cannas,[1] Luciano Cascione,[1,3] Eugenio Gaudio,[1] Alberto J. Arribas,[1,3] Shivaprasad Manjappa,[4] Gaetanina Golino,[1] Lorenzo Scalise,[1] Maria Teresa Cacciapuoti,[5] Emanuele Zucca,[1,6] Anastasios Stathis,[6,7] Giorgio Inghirami,[5] Patrick H. van Berkel,[8] Davide Rossi,[1,6] Paolo F. Caimi,[9] Francesca Zammarchi[8] and Francesco Bertoni[1,6]

[1]Institute of Oncology Research, Faculty of Biomedical Sciences, USI, Bellinzona, Switzerland; [2]Case Western Reserve University, Cleveland, OH, USA; [3]SIB Swiss Institute of Bioinformatics, Lausanne, Switzerland; [4]Fred Hutchinson Cancer Center, Seattle, WA, USA; [5]Department of Pathology and Laboratory Medicine, Weill Cornell Medicine, New York, NY, USA; [6]Oncology Institute of Southern Switzerland, Ente Ospedaliero Cantonale, Bellinzona, Switzerland; [7]Faculty of Biomedical Sciences, USI, Lugano, Switzerland; [8]ADC Therapeutics (UK) Ltd., London, UK and [9]Cleveland Clinic/Case Comprehensive Cancer Center, Cleveland, OH, USA

*CT and DW contributed equally as first authors.

Correspondence: C. Tarantelli
chiara.tarantelli@ior.usi.ch

F. Bertoni
francesco.bertoni@ior.usi.ch

Targeting CD19-positive lymphomas with the antibody-drug conjugate loncastuximab tesirine: preclinical evidence as single agent and in combination therapy

Chiara Tarantelli* [1^], David Wald [2^], Nicolas Munz [1], Filippo Spriano [1], Alessio Bruscaggin [1], Eleonora Cannas [1], Luciano Cascione [1,3], Eugenio Gaudio [1], Alberto J. Arribas [1,3], Shivaprasad Manjappa [4], Gaetanina Golino [1], Lorenzo Scalise [1], Maria Teresa Cacciapuoti [5], Emanuele Zucca [1,6], Anastasios Stathis [6,7], Giorgio Inghirami [5], Patrick H. van Berkel [8], Davide Rossi [1,6], Paolo F. Caimi [9], Francesca Zammarchi [8], Francesco Bertoni* [1,6]

[1] *Institute of Oncology Research, Faculty of Biomedical Sciences, USI, Bellinzona, Switzerland;*
[2] *Case Western Reserve University, Cleveland, OH, USA;*
[3] *SIB Swiss Institute of Bioinformatics, Lausanne, Switzerland;*
[4] *Fred Hutchinson Cancer Center, Seattle, Washington, USA;*
[5] *Department of Pathology and Laboratory Medicine, Weill Cornell Medicine, New York, NY;*
[6] *Oncology Institute of Southern Switzerland, Ente Ospedaliero Cantonale, Bellinzona, Switzerland;*
[7] *Faculty of Biomedical Sciences, USI, Lugano, Switzerland;*
[8] *ADC Therapeutics (UK) Ltd., London, UK;*
[9] *Cleveland Clinic/Case Comprehensive Cancer Center, Cleveland, OH, USA.*

Supplementary materials and methods

Cell lines

Lymphoma cell lines were cultured according to the recommended conditions, as previously described [1]. All media were supplemented with fetal bovine serum (10% or 20%) and penicillin-streptomycin-neomycin (≈5,000 units penicillin, 5 mg streptomycin, and 10 mg neomycin/mL; Sigma). Human cell line identities were confirmed by short tandem repeat DNA fingerprinting using the Promega GenePrint 10 System kit (B9510). Cells were periodically tested for mycoplasma negativity using the MycoAlert Mycoplasma Detection Kit (Lonza).

Compounds

Loncastuximab tesirine, SG3199 and B12-SG3249 were provided by ADC Therapeutics. Copanlisib was purchased from MedKoo Biosciences Inc. (Morrisville, NC, USA). Idelalisib, venetoclax, bendamustine, olaparib, ibrutinib, doxorubicin, vincristine, prednisolone, bortezomib, and lenalidomide were purchased from Selleckchem (Houston, TX, USA). Rituximab was purchased from Roche (Basel, Switzerland), and 4-hydroperoxy-cyclophosphamide from Santa Cruz Biotechnology (Heidelberg, Germany).

Patient-derived xenograft (PDX) cell line

PDX was first digested and then passed through 70μm nylon filters. Cell suspension was washed twice with PBS, and dead cells were removed using the Ficoll gradient. Viable cells were then cultured in RPMI (Sigma) supplemented with 20% FBS (Corning), 100 U/ml glutamine (Sigma), Normocin 1:500 (InvivoGen), and 100μg/ml streptomycin (Sigma) and maintained at 37°C in a humidified 5% CO2 atmosphere [2]. PDX-Dlines media was initially supplemented with exogenous IL-2 (50U/ml), IL6 (10μg/ml), and IL10 (20μg/ml). Exogenous lymphokines were ultimately excluded when possible. PDX-Dline was analyzed by flow cytometry using a panel of monoclonal antibodies against human pan B- or T-cell surface markers twice per year. Genotyping was performed once a year (biosynthesis, Tx). PDX was produced in the context of protocols approved by the Cornell University (IRB: 107004999, 0201005295 and 1410015560; Universal consent: 1302013582; *in vivo* protocol 2014-0024).

To determine the expression of CD19, 1x106 cells were pre-incubated with FcR blocking reagent (catalog no. 130-059-901; Miltenyi Biotec, Bisley, UK) to prevent unspecific binding of staining antibodies, following manufacturer's instructions, and then stained with anti-Hu-CD19 antibody (BD Biosciences, BD Pharmingen PE Mouse Anti-human CD19-555413) or with the isotype (BD Pharminge PE Mouse IgG1, κ Isotype Control-555749). Median Fluorescence Intensities were acquired in a BD

LSRFortessa instrument (BD Biosciences, Allschwil, Switzerland), and data were analyzed using FlowJo software (TreeStar Inc., Ashland, OR USA).

LyV4.0 CAPP-seq gDNA Assay and variant calling

Genomic DNA was extracted from cell lines using the DNeasy Blood & Tissue Kits (Qiagen, Hilden, Germany). Library preparation started with shearing at least 500 ng of DNA through sonication (Covaris, Woburn, MA) to obtain 100 to 200 bp fragments. The gDNA libraries were then generated with the KAPA Hyper Prep Kit (KAPA Biosystems). The regions of interest (Table S1) were enriched using SeqCap HyperChoice Library probes (NimbleGen; Roche Diagnostics, Jakarta, Indonesia). Libraries were sequenced on the NextSeq500 (Illumina, San Diego, CA) instrument by paired-end sequencing (2 × 150-cycle protocol). A total of 52 multiplexed libraries were simultaneously sequenced in each deep experiment. Sequencing reads in FASTQ format were deduplicated utilizing FastUniq v1.1. The resulting reads were locally aligned to the hg19 human genome assembly using the BWA-MEM v.0.7.17 software with the default settings and then sorted, indexed, and assembled into a mpileup file using SAMtools v.1.7. The aligned reads were processed with mpileup using the parameters -A -d 10 000 000. Single nucleotide variations and indels were called in gDNA with the mpileupCNS function of VarScan2 (v.2.2.4) using the parameters min-coverage 1 --min-coverage-normal 1 --min-coverage-tumor 1 --min-var-freq 0 --min-freq-for-hom 0.75 --somatic-p-value 0.05 --min-avg-qual 30 --strand-filter 1 --validation 1 --output VCF. The variant called by VarScan2 was annotated using the Annovar software (wAannovar https://wannovar.wglab.org/). The analysis retained all the variants affecting coding regions or splice sites. All variants were systematically compared to online databases to confer the origin of somatic status. Somatic origin of non-synonymous single nucleotide variants (SNV) and/or inframe In/del was confirmed only if was detected as "somatic confirmed" in COSMIC database (https://cancer.sanger.ac.uk/cosmic), without a presence in polymorphisms database (https://www.ncbi.nlm.nih.gov/variation/view/ ; https://www.ncbi.nlm.nih.gov/variation/tools/1000genomes/); somatic status was also confirmed by the high damaging prediction score provided by poliphen2 and SIFT online software (http://genetics.bwh.harvard.edu/pph2/ ; https://sift.bii.a-star.edu.sg/www/SIFT4G_vcf_submit.html). Their non-presence in the polymorphisms' database was enough to call variants somatic for truncating variants, frameshift, splicing variants, and/or stop codons. An in-house database containing all gDNA background allele frequencies across gDNA samples from healthy subjects was used to filter out systematic sequencing errors in gDNA. Based on the assumption that all background allele fractions follow a normal distribution, a Z-test was employed to test whether a given variant in the gDNA differed significantly in its frequency from typical gDNA background at the same position in all gDNA samples after adjusting for multiple comparisons by Bonferroni test (multiple comparisons corrected p threshold corresponding to alpha of 0.05/[size of the target region in bp × 4 alleles per position]). Variants that did not pass these filters were not further considered. Variants for the resulting candidate mutations were visualized using Integrative Genomics Viewer. Genes mutational levels were correlated with loncastuximab tesirine drug activity quantified as IC_{50} values by Mann Whitney test with STATA Stata/BE 17.0 (Stata Corporation, College Station, TX). P-value for significance was <0.05. For multiple correction analysis, a two-stage linear step-up procedure of Benjamini, Krieger, and Yekutieli was adopted with significance at a threshold of <0.05, using Prism software v8.0 (GraphPad Software La Jolla, CA, USA).

Immunoblotting

Cells were seeded in T25 flasks at a density of $5x10^5$ per mL and treated for 24 hours with DMSO or single drugs at their 2 times IC_{50} concentrations or with loncastuximab tesirine plus venetoclax, idelalisib, or copanlisib. Protein extraction was performed by lysing the cells with M-PER (Mammalian Protein Extraction Reagent, ThermoFisher Scientific, Waltham, MA, USA) lysis buffer plus Halt Protease and Phosphatase Inhibitor Cocktail, EDTA-Free (100X) for 30 minutes on ice and then centrifuged at high speed and 4°C for 30 minutes. Protein concentration was determined using the BCA protein assay (Pierce Chemical Co, Dallas, TX, USA), and 30 µg of total proteins were loaded and

separated on a 4-20% gradient SDS-polyacrylamide gel by electrophoresis (SDS-PAGE). Proteins were transferred on nitrocellulose membranes and incubated with primary antibodies overnight, followed by the appropriate horseradish peroxidase–conjugated anti-mouse (NA931V) or anti-rabbit (NA934V) secondary antibodies (GE Healthcare, Chicago, IL, USA) for 1 hour at room temperature. Enhanced chemiluminescence detection was done following the manufacturer's instructions (Amersham Life Science). Luminescence is measured by the Fusion Solo S instrument (Witec AG, Sursee, Switzerland). Finally, protein quantification was performed using the Fusion Solo S instrument (Witec AG). Equal loading of samples was confirmed by probing for vinculin. The antibodies used for the experiment were: anti-Vinculin (Sigma Aldrich cat. n.V9131), anti-AKT (CST-9272), anti-p-AKT (Ser 473) (CST-4060), anti-CD19 (abcam-AB134114), anti-PARP1 (SC-8007), anti-Mcl1 (D35A5) (CST-5453) and anti-Bcl2 (SC-492) as primary antibodies.

Cell cycle

Cells were seeded in 96 wells-plates at a density of 10^4 (OCI-LY-3) or 2×10^4 (TMD8, VAL, WSU-DLCL2) per well and subsequently treated with single drugs or with the combination of loncastuximab tesirine plus venetoclax, idelalisib or copanlisib at 2 times IC_{50} concentrations for 96 hours. Cells were fixed with 70% cold ethanol before staining with propidium Iodide (PI) and RNAse treatment. Acquisitions were carried out with a FACSCanto II instrument (BD Biosciences, Allschwil, Switzerland), and data were analyzed using FlowJo software (TreeStar Inc., Ashland, OR, USA).

Data mining

Statistical analyses were conducted using Prism software v8.0 (GraphPad Software La Jolla, CA, USA). For immunoblotting, cell proliferation, cell death, cell cycle, and apoptotic assay, statistical significance was determined by a two-tailed unpaired Student's t-test. A P value < 0.05 was considered statistically significant. *BCL2* and/or *MYC* translocations and *TP53* inactivation were retrieved from our previous publication [3]. Differences in IC_{50} values among lymphoma subtypes were calculated using the Mann-Whitney test. P values of 0.05 or less defined statistical significance.

In vivo experiments

TMD8 xenograft: Mice maintenance and animal experiments were performed under the institutional guidelines established for the Animal Facility at The Institute of Research in Biomedicine (IRB) (license n. TI 49-2018). NOD-SCID mice were obtained from Charles River (Wilmington, MA, USA). Xenografts were established by injecting TMD8 lymphoma cells (15×10^6 cells/mouse, 200 µL of PBS) into the left flanks of female NOD-SCID mice (6 weeks of age, approximately 20 grams of body weight). Treatments started with measurable tumors. Tumor volume (TV) was calculated using the equation V = [length x width x height]/2. The animal status was evaluated during housing and treatments by measuring the Body Condition Score (BSC) [4].

JEKO1 xenograft: Eight-week-old female Nod/SCID/IL2-Rg-/- (NSG) mice (Jackson Lab, Bar Harbor, Maine) were injected subcutaneously into both flanks with 10×10^6 Jeko1 cells. Mice were sacrificed according to institutional guidelines (signs of significant disease morbidity such as limb paralysis or greater than 20% weight loss). Animal experiments were approved and performed following the policies and regulations set forth by the Institutional Animal Care and Use Committee of Case Western Reserve University.

In combination experiments, statistical significances between groups were defined using the Mann-Whitney test followed by a two-stage step-up (Benjamini, Krieger, and Yekutieli) multiple comparisons, FDR=1%. The coefficient of drug interaction (CDI) [5] was used to assess the additive (CDI = 1), supra-additive (synergism, CDI < 1), or sub-additive (CDI > 1) effect of the treatment versus the control arms, as previously performed [6]. In single-treatment experiments, differences between tumor volumes were considered statistically significant using the Mann-Whitney test, P<0.05.

References

1.   Johnson Z, Tarantelli C, Civanelli E, et al. IOA-244 is a Non-ATP-competitive, Highly Selective, Tolerable PI3K Delta Inhibitor That Targets Solid Tumors and Breaks Immune Tolerance. Cancer Res Commun. 2023;3(4):576-591.

2.   Cappelli LV, Fiore D, Phillip JM, et al. Endothelial cell-leukemia interactions remodel drug responses, uncovering T-ALL vulnerabilities. Blood. 2023;141(5):503-518.

3.   Tarantelli C, Gaudio E, Arribas AJ, et al. PQR309 Is a Novel Dual PI3K/mTOR Inhibitor with Preclinical Antitumor Activity in Lymphomas as a Single Agent and in Combination Therapy. Clin Cancer Res. 2018;24(1):120-129.

4.   Ullman-Culleré MH, Foltz CJ. Body condition scoring: a rapid and accurate method for assessing health status in mice. Lab Anim Sci. 1999;49(3):319-323.

5.   Wu J, Tracey L, Davidoff AM. Assessing interactions for fixed-dose drug combinations in tumor xenograft studies. J Biopharm Stat. 2012;22(3):535-543.

6.   Jabeen A, Huang S, Hartley JA, Van Berkel PH, Zammarchi F. Combination of Camidanlumab Tesirine, a CD25-Targeted ADC, with Gemcitabine Elicits Synergistic Anti-Tumor Activity in Preclinical Tumor Models. Blood. 2020;136(Supplement 1):31-32.

Supplementary Figure and Tables

Supplementary Tables

Table S1. **Regions specifically sequenced by the probes in the targeted DNA-sequencing data.**
Each row delineates the primary target of genomic spaces covered by the probes according to the Hg19 genome reference. [See excel file]

Table S2. IC$_{50}$ values obtained in lymphoma cell lines after 96 hours of exposure to loncastuximab tesirine, SG3199 and isotype-control ADC (B12-C220-SG3249), in addition to CD19 surface protein expression in lymphoma cell lines as measured following an absolute fluorescence quantitation with Quantum Simply Cellular microspheres using rB4v1.2 antibody.
DLBCL, diffuse large B-cell lymphoma; ABC, activated B cell; GCB, germinal center B cell; MCL, mantle cell lymphoma; MZL, marginal zone lymphoma; CLL, chronic lymphocytic leukemia; PMBCL, primary mediastinal large B cell lymphoma; CTCL, cutaneous T cell lymphoma; ALCL, anaplastic large cell lymphoma; PTCL-NOS, peripheral T cell lymphoma-not otherwise specified; HL, Hodgkin lymphoma.

HISTOLOGY	CELL LINE	LONCASTUXIMAB TESIRINE (IC$_{50}$, PM)	SG3199 (IC$_{50}$, PM)	RB4V1.2 NORMALIZED ANTIBODY BINDING CAPACITY	B12-C220-SG3249 (IC$_{50}$, PM)
ABC DLBCL	HBL-1	12.1	1.2	57597	2500
ABC DLBCL	OCI-Ly-3	10	0.8	29163	1200
ABC DLBCL	RCK8	35	1.2	88579	2500
ABC DLBCL	RI-1	45	5.8	44683	3162.5
ABC DLBCL	SU-DHL-2	400	1.1	10896	1300
ABC DLBCL	TMD8	6	0.5	42808	550
ABC DLBCL	U2932	1100	8.8	51776	5562.5
GCB DLBCL	DB	100	3.2	100060	300
GCB DLBCL	DOHH2	0.5	0.5	15703	125
GCB DLBCL	FARAGE	2	0.9	132705	1650
GCB DLBCL	KARPAS 422	31.1	5.3	147515	8000
GCB DLBCL	OCI-Ly-1	1.4	1.4	17514	275
GCB DLBCL	OCI-Ly-18	0.6	0.5	0	150
GCB DLBCL	OCI-Ly-19	0.8	0.5	87842	175
GCB DLBCL	OCI-Ly-7	1.4	1.1	68590	2250
GCB DLBCL	OCI-Ly-8	0.3	0.5	58172	90
GCB DLBCL	PFEIFFER	790	14.6	77045	25000
GCB DLBCL	SU-DHL-10	2.8	0.9	51975	750
GCB DLBCL	SU-DHL-16	2812.5	1.1	25787	2500
GCB DLBCL	SU-DHL-4	9.5	1.4	176138	2250
GCB DLBCL	SU-DHL-5	2	0.8	56953	650
GCB DLBCL	SU-DHL-6	6.3	14.6	63374	9500
GCB DLBCL	SU-DHL-8	1.5	1.2	66635	2500
GCB DLBCL	TOLEDO	13	1.4	75346	2812.5
GCB DLBCL	VAL	0.4	0.5	74808	340
GCB DLBCL	WSU-DLCL2	3	1.8	9848	1500

PMBCL	KARPAS 1106P	1.5	0.6	126819	690
MCL	GRANTA519	1.4	0.5	50553	400
MCL	JEKO1	5.3	0.5	45616	2250
MCL	JVM2	5.5	2.0	47160	3000
MCL	MAVER1	2.8	0.7	98854	900
MCL	MINO	1	0.5	115483	450
MCL	REC1	20000	32.2	80734	32500
MCL	SP49	1.3	0.5	40871	700
MCL	SP53	2	0.5	72511	850
MCL	UPN1	0.9	0.8	50600	600
MCL	Z138	1.5	0.5	22049	300
CLL	MEC1	5.5	0.5	92461	1800
CLL	PCL-12	26	1.1	60314	2562.5
MZL	ESKOL	3	0.5	51311	650
MZL	HAIR-M	9.5	0.8	52925	900
MZL	HC1	0.5	0.5	58951	200
MZL	KARPAS 1718	0.7	0.5	36730	400
MZL	SSK41	2	0.8	20233	650
MZL	VL51	550	0.5	7497	450
HL	AM-HLH	600	0.8	0	300
HL	KM-H2	2750	5.0	219	5250
HL	L-428	14000	29.2	0	13750
PTCL-NOS	FE-PD	850	0.5	0	750
ALCL	KARPAS 299	11500	17.5	0	12500
ALCL	KI-JK	4000	3.5	0	2962.5
ALCL	L-82	5750	1.2	0	5500
ALCL	SU-DHL-1	700	0.8	0	600
CTCL	MAC1	900	0.5	0	1500
CTCL	H9	1500	2.3	0	900
CTCL	HH	35000	23.4	0	24000
CTCL	HUT-78	3500	0.8	0	1700
Canine B cell lymphoma	CLBL1	175	0.5	0	175
Murine B cell lymphoma	A20	2012.5	1.0	0	850
Murine B cell lymphoma	BCL1 clone 5B1b	500	0.5	0	435

Table S3. IC$_{50}$ values obtained in DLBCL cell lines after 72 hours exposure to R-CHOP.

CELL LINE	R-CHOP (IC50 UG/ML)
DB	0.0476
DOHH2	0.0150
FARAGE	0.0009
HBL-1	0.0748
KARPAS 422	0.0573
OCI-LY-1	0.0066
OCI-LY-18	0.0529
OCI-LY-19	0.0097
OCI-LY-3	0.0123
OCI-LY-7	0.0082
OCI-LY-8	0.0006
PFEIFFER	0.1471
RCK8	0.0431
RI-1	0.8127
SU-DHL-10	0.0007
SU-DHL-16	0.1338
SU-DHL-2	0.2383
SU-DHL-4	0.0113
SU-DHL-5	0.0134
SU-DHL-6	0.0029
SU-DHL-8	0.0569
TMD8	0.0134
TOLEDO	0.0771
U2932	0.1542
VAL	0.0003
WSU-DLCL2	0.2056

Table S4. **Mutational analysis in B cell lymphoma cell lines.** Mapping based on the Hg19 genome reference. [See excel file]

Supplementary figures

Figure S1. Distribution of IC$_{50}$ values of loncastuximab tesirine (ADCT-402) between B and T-cell lymphoma derived cell lines. ****, P<0.0001 as determined by the Mann-Whitney test.
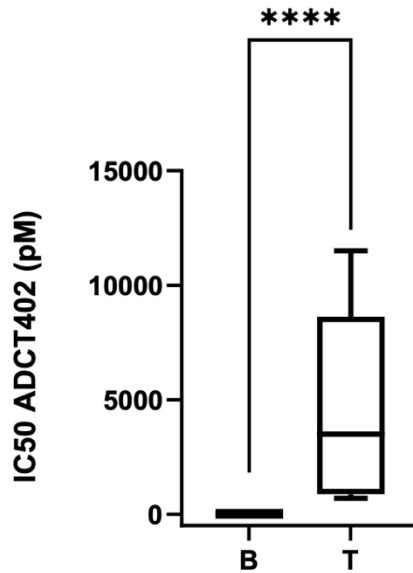
Figure S2. Representative images of the apoptosis induction in two DLBCL cell lines exposed to loncastuximab tesirine (ADCT-402) and analyzed for annexin V by flow cytometry. Cells were treated (2 x IC50) for 96 hours. The frequencies of annexin V positive cells (early apoptotic cells), annexin V/ propidium iodide double positive (late apoptosis), necrotic (annexin V negative, propidium iodide positive) and alive cells (annexin V/propidium iodide double negative) are shown.
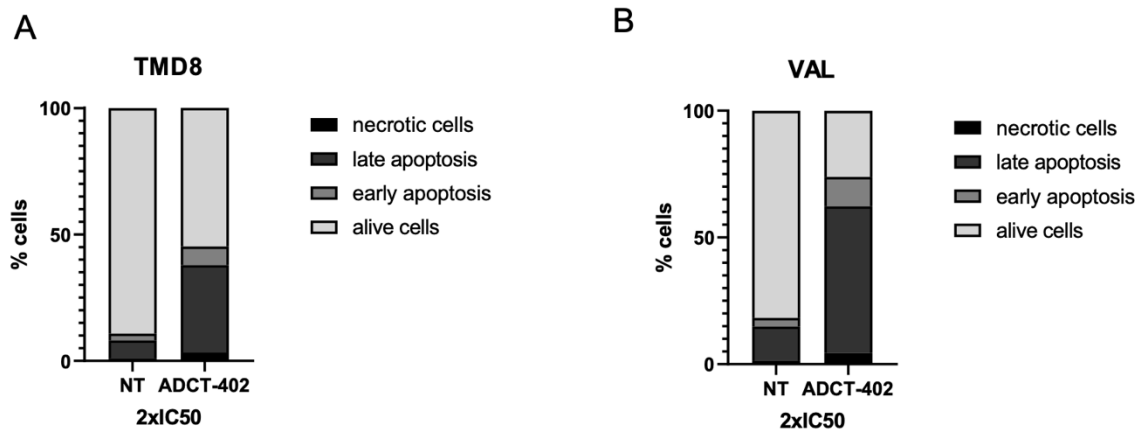
Figure S3. Distribution of IC$_{50}$ values of loncastuximab tesirine among DLBCL cell lines based on the presence or absence of BCL2 and MYC chromosomal translocations as single or concomitant events (double hit) and of TP53 status. A) DLBCL cell lines with (n=16) and without (n=7) *TP53* inactivation. B) DLBCL cell lines with (n=15) and without (n=11) *BCL2* translocation. C) DLBCL cell lines with (n=7) and without (n=19) concomitant *BCL2* and *MYC* translocation. D) DLBCL cell lines with (n=10) and without (n=16) *MYC* translocation. *, P< 0.05; **, P< 0.001.
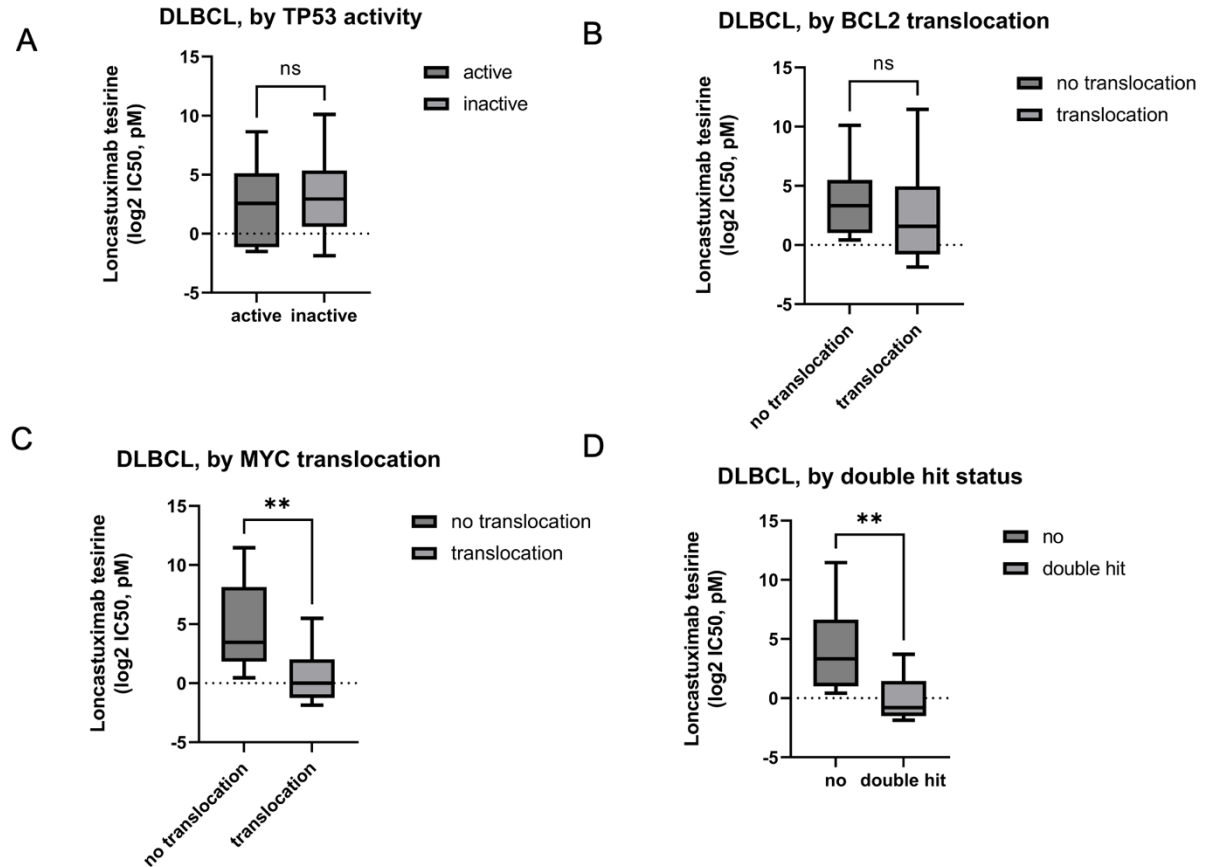
Figure S4. MYC, CD19, and IC$_{50}$ values of loncastuximab tesirine among DLBCL cell lines. A) CD19 surface expression between cell lines with and without MYC translocation. B) CD19 RNA expression values measured via RNA-Seq between cell lines with and without MYC translocation. C) CD19 RNA expression values measured via microarray between cell lines with and without MYC translocation. D) correlation plot between CD19 surface expression and MYC expression measured via RNA-Seq. E) correlation plot between CD19 RNA and MYC expression, both measured via RNA-Seq. F) Correlation between loncastuximab tesirine IC$_{50}$ values and MYC expression measured via RNA-Seq.
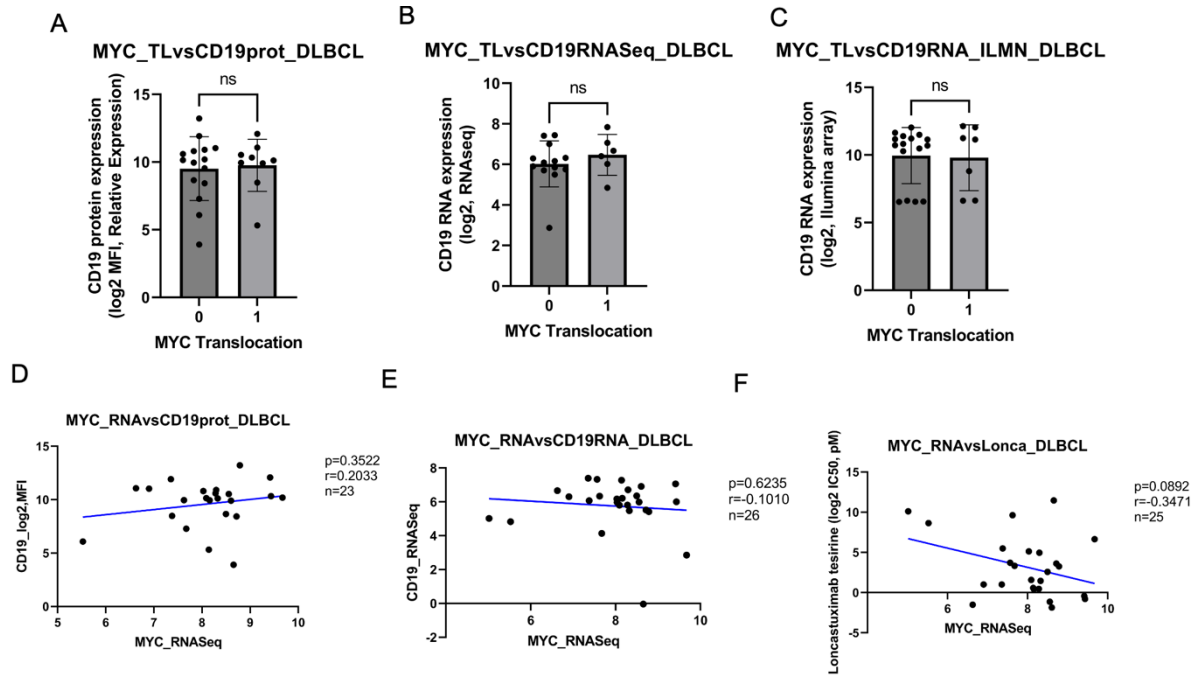
Figure S5. Distribution of IC$_{50}$ values of SG3199 between B and T derived lymphoma cell lines.
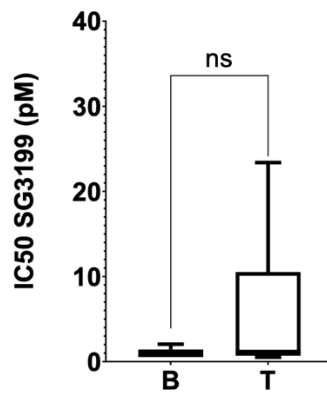
Figure S6. Pearson correlation between SG3199 and CD19 absolute expression among B cell lymphoma cell lines.
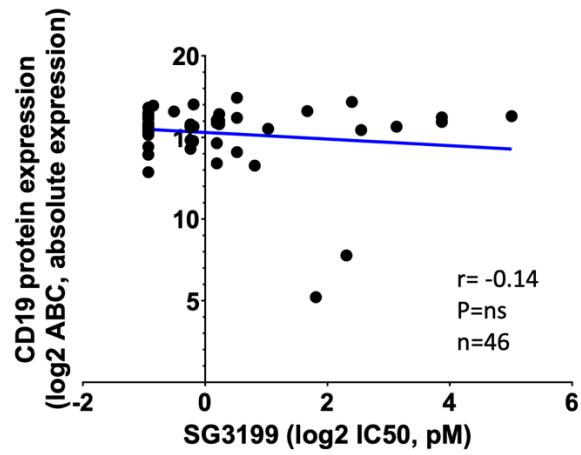
Figure S7. Distribution of IC$_{50}$ values of loncastuximab tesirine and SG3199 across all cell lines (A) and among B cell lymphoma cell lines (B). ****, P<0.0001 as determined by the Mann-Whitney test.
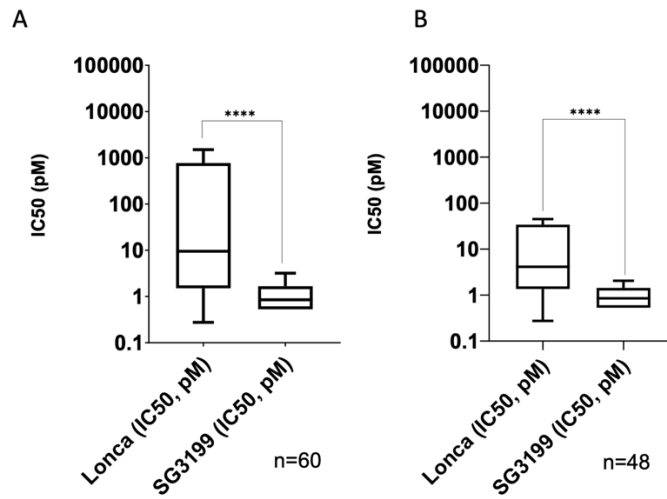
Figure S8. Distribution of IC$_{50}$ values of SG3199 among DLBCL cell lines based on the presence or absence of BCL2 and MYC chromosomal translocations as single or concomitant events (double hit) and of TP53 status. A) DLBCL cell lines with (n=16) and without (n=7) *TP53* inactivation. B) DLBCL cell lines with (n=15) and without (n=11) *BCL2* translocation. C) DLBCL cell lines with (n=7) and without (n=19) concomitant *BCL2* and *MYC* translocation. D) DLBCL cell lines with (n=10) and without (n=16) *MYC* translocation. *, P< 0.05; **, P< 0.001.
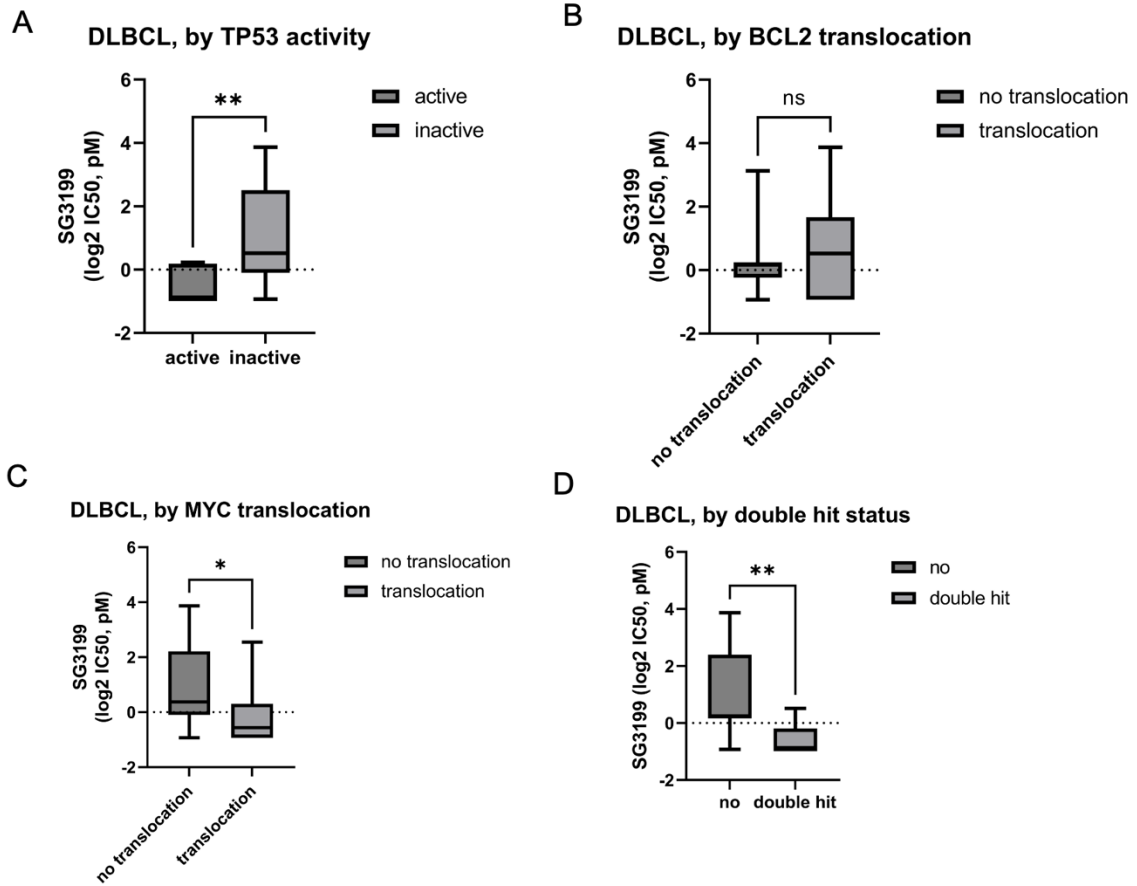
Figure S9. Pearson correlation between SG3199 IC$_{50}$ values and MYC RNA levels measured via RNA-Seq (A) and via microarray (B) among DLBCL cell lines.
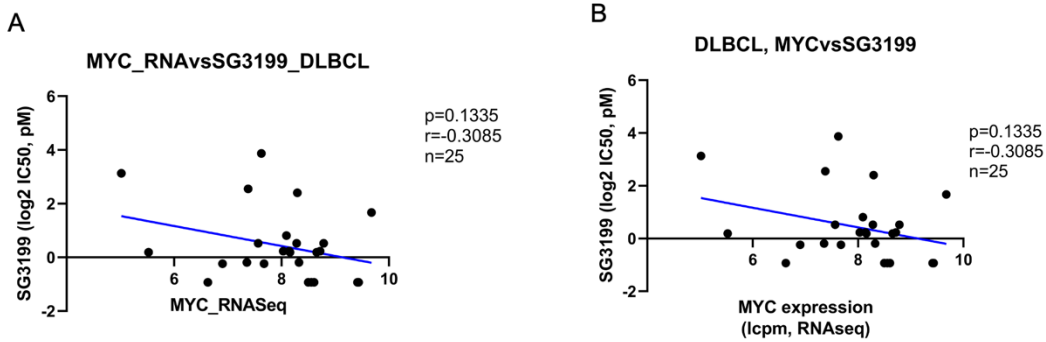
Figure S10. SU-DHL-6 cell line is sensitive to loncastuximab tesirine and to its naked antibody, but it is resistant to its warhead SG3199. Loncastuximab tesirine, SG3199, and rB4v1.2 activity was evaluated by MTT assay for 96 hours of treatment. X axis, concentration in pM; Y axis, fold to untreated. * q values < 0.05 of loncastuximab tesirine vs all other treatments (SG3199, rB4v1.2) was determined by unpaired t-test followed by two-stage step-up (Benjamini, Krieger, and Yekutieli) multiple comparisons, FDR(q)=0.05.
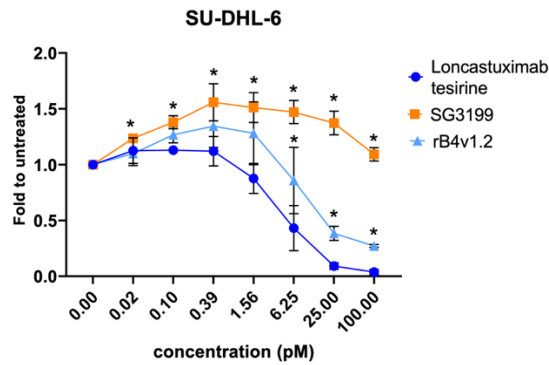
Figure S11. Correlation between in vitro antiproliferative activities of loncastuximab tesirine and two others anti-CD19 ADCs. Pearson correlations between log2 IC$_{50}$ (pM) of loncastuximab tesirine activity with coltuximab ravtansine (SAR34199) (A) or huB4-DGN462 (B).
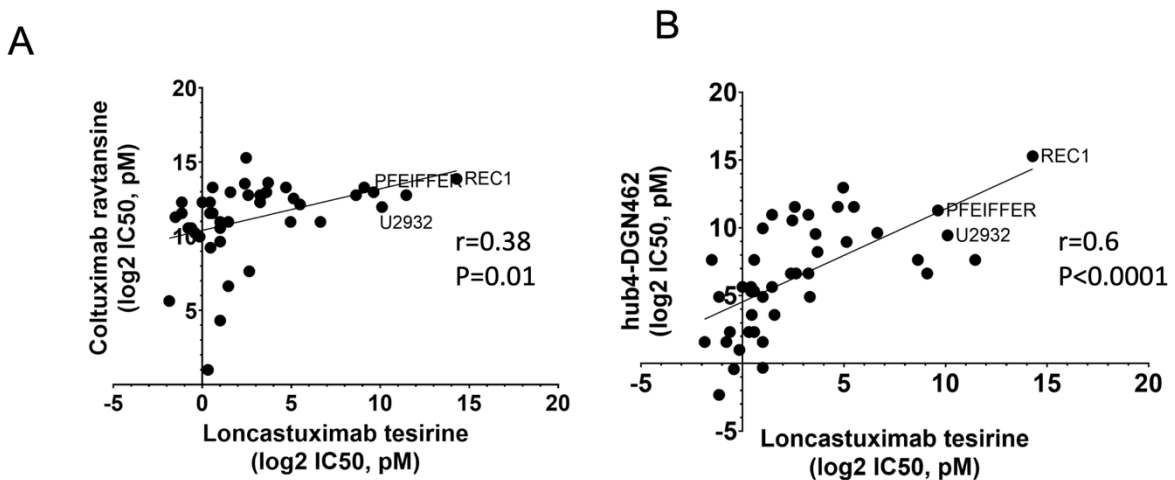
Figure S12. Cell cycle distribution of DLBCL cell lines after 96h of treatment with loncastuximab tesirine alone or in combination with venetoclax, idelalisib or copanlisib. TMD8 (A), WSU-DLCL2 (B), OCI-LY-3 (C) and VAL (D) were treated with two times IC_{50}. Statistics were calculated with the Student's t-test. *P value < .05. Single asterisk compares exposure conditions with the untreated sample.
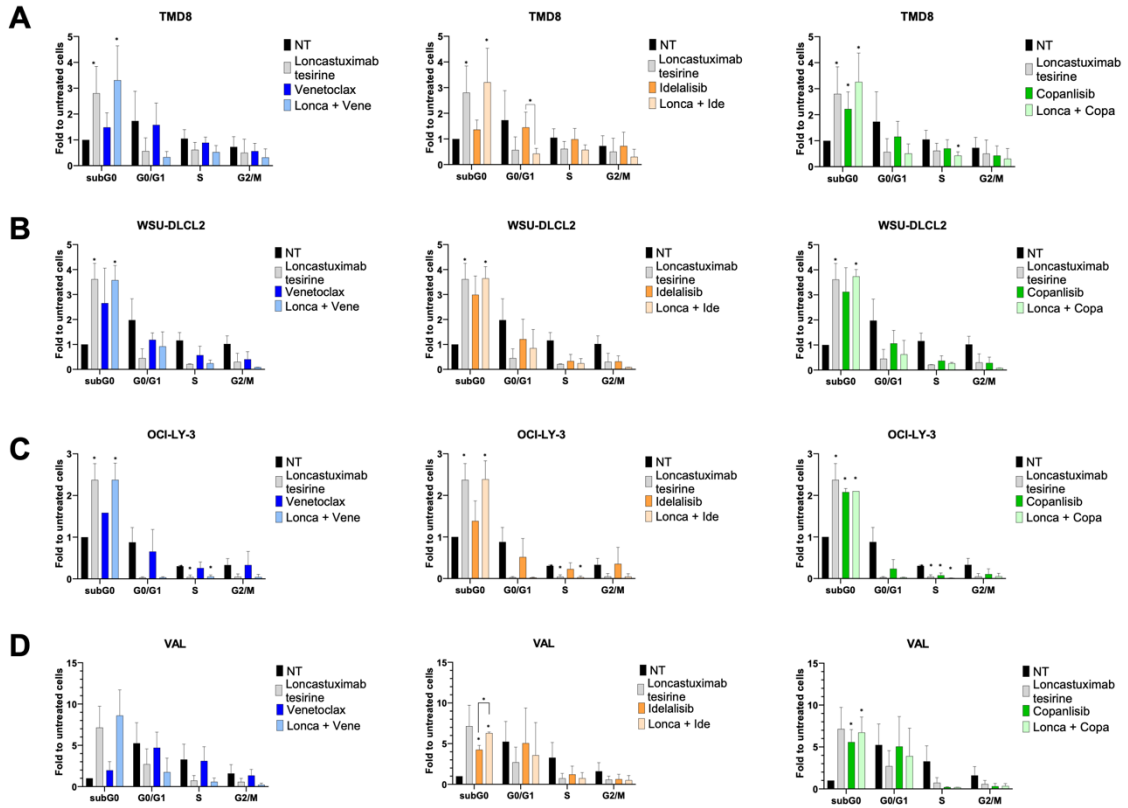
Figure S13. Quantification of protein changes in cells treated with loncastuximab tesirine as a single agent or in combination with venetoclax, idelalisib, and copanlisib.
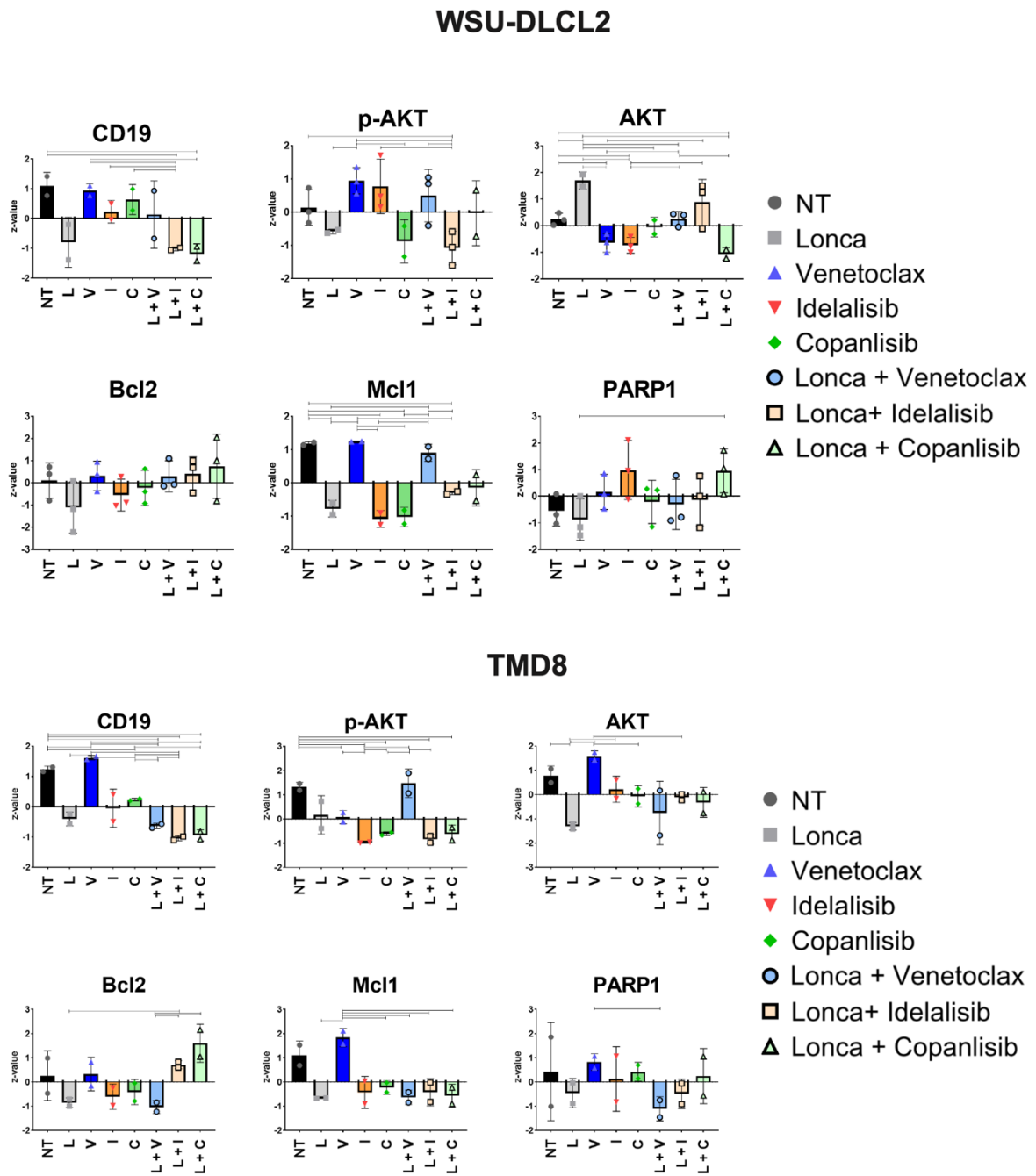
Figure S14. PDX-derived lymphoma cells from one patient resistant to CD19 targeting CART cells are sensitive to loncastuximab tesirine. (A) PDX-derived lymphoma cells from one patient resistant to CD19 targeting CART cells were left unstained and stained with anti-human-CD19-PE and isotype-PE, and then flow cytometry was performed. The number of events (count), median PE-value, and Frequency of PE-positive cells are shown in the figure. MTT results are shown in **B** and **C.** Cells were treated with the necked antibody rB4v1.2, the isotype associated with the toxin (B12-C220-SG3249), loncastuximab tesirine and the toxin SG3199 at increased doses for 96 hours.
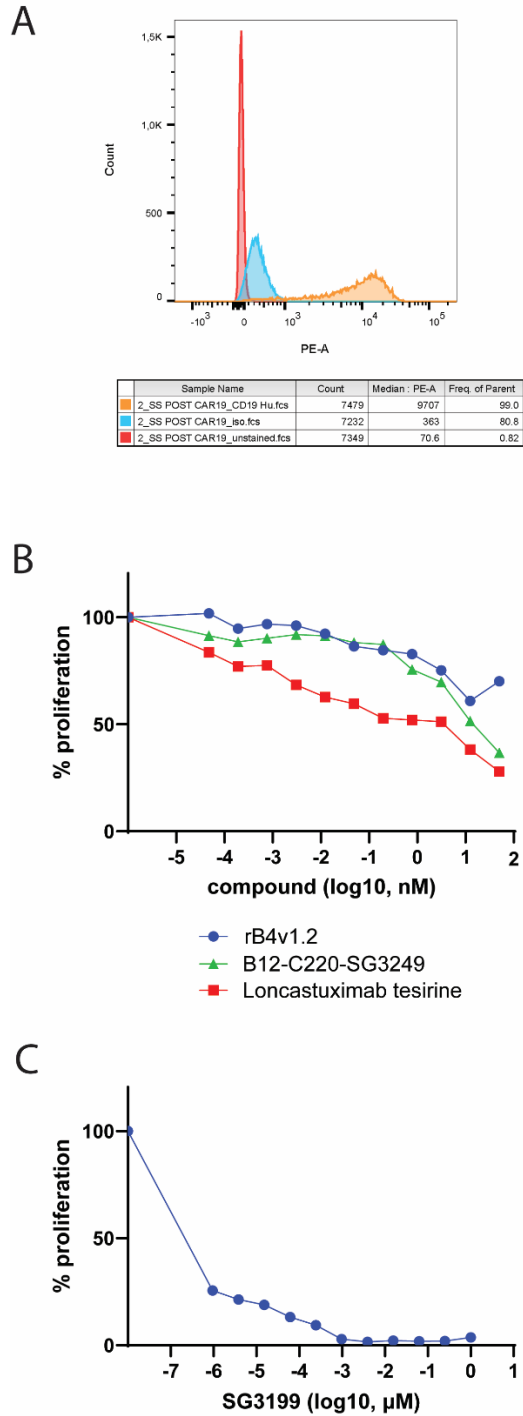
Figure S15. Single agent in vivo activity of loncastuximab tesirine and B12-SG3249 in TMD8 ABC DLBCL.
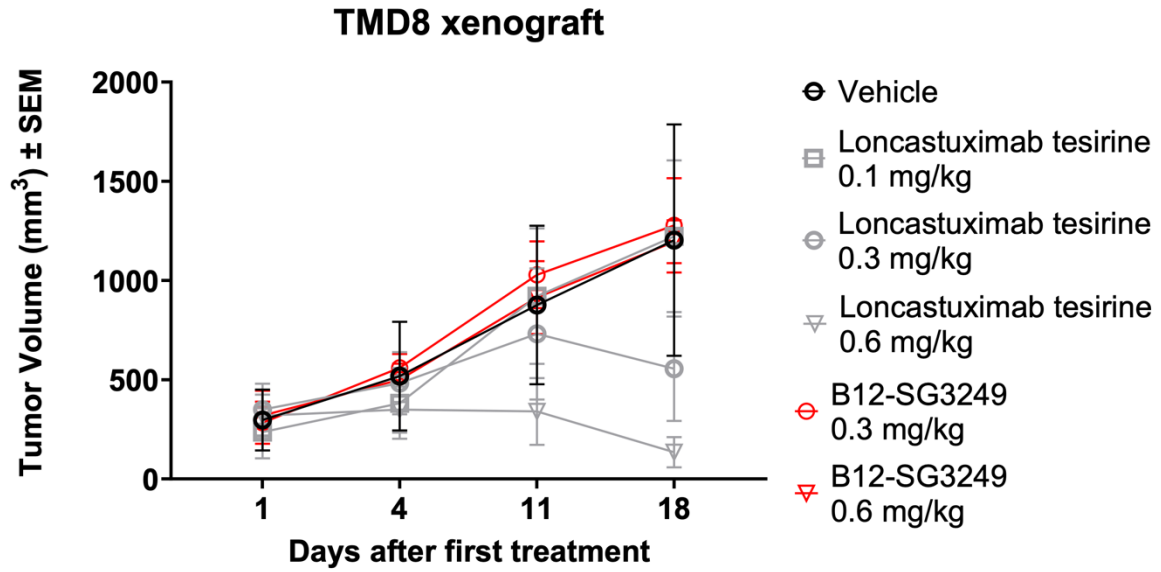
Figure S16. Single agent in vivo activity of copanlisib in TMD8 ABC DLBCL. * p values < 0.05 of copanlisib (both dosages) vs vehicle, as determined by Mann-Whitney test.
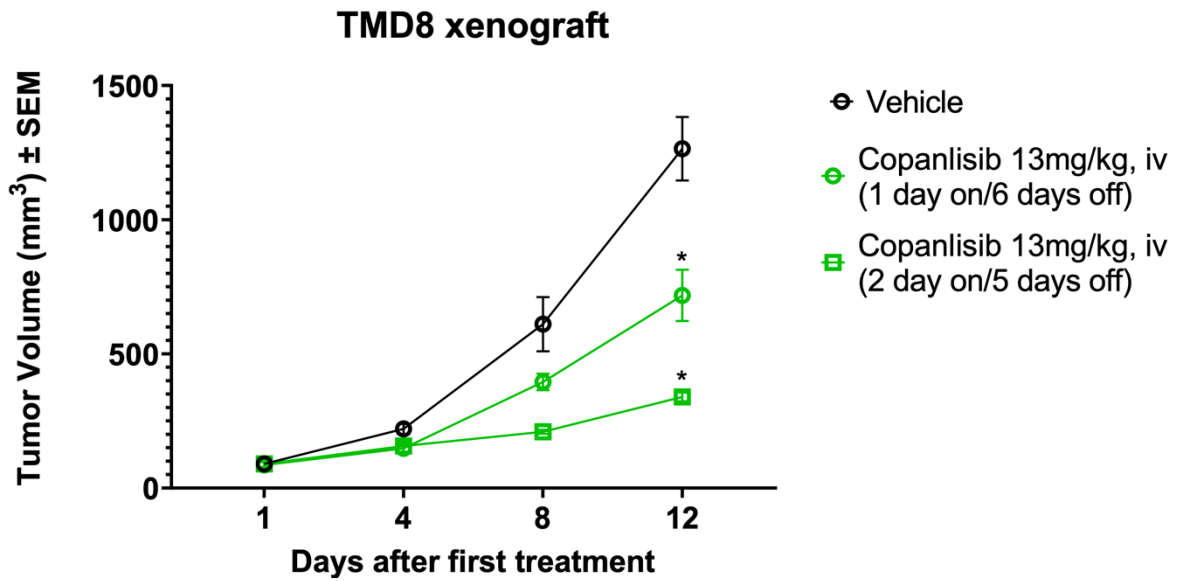
Figure S17. Tumor weight in grams of xenografts from mice treated with loncastuximab tesirine in combination with copanlisib (TMD8) (A) or venetoclax (Jeko1) (B). *, P<0.05; **, P<0.005; ***, P<0.0001 as determined by the Mann-Whitney test.